

Uniaxial strain effect in a strongly correlated two-dimensional system $\beta'-(\text{CH}_3)_4\text{As}[\text{Pd}(\text{dmit})_2]_2$

Reizo Kato,* Naoya Tajima, and Masafumi Tamura

RIKEN (The Institute of Physical and Chemical Research), 2-1, Hirosawa, Wako-shi, Saitama, 351-0198, Japan

Jun-Ichi Yamaura

The Institute for Solid State Physics, The University of Tokyo, 5-1-5 Kashiwanoha, Kashiwa-shi, Chiba 277-8581, Japan

(Received 10 May 2002; published 16 July 2002)

The molecular conductor $\beta'-(\text{CH}_3)_4\text{As}[\text{Pd}(\text{dmit})_2]_2$ (dmit=1,3-dithiol-2-thione-4,5-dithiolate) is a two-dimensional system based on the dimer structure. At low temperature, this system is a Mott insulator under ambient and hydrostatic pressure conditions. The electrical resistivities of this system have been measured under uniaxial strain along all three crystallographic axes. When the strain is applied parallel to the b axis within the a - b conducting layer, the nonmetallic behavior is readily suppressed and superconductivity appears at 4 K under 7 kbar. On the other hand, small strain around 2 kbar along both the a - and c -axis directions effectively enhances the nonmetallic behavior. With further increase of the strain, the nonmetallic behavior is suppressed, but cannot be removed even at 15 kbar. These unusual results suggest the crucial role of intra- and interdimer interactions that affect the band width and the effective on-site Coulomb interaction.

DOI: 10.1103/PhysRevB.66.020508

PACS number(s): 74.70.Kn, 71.20.Rv, 71.30.+h

The electronic states of molecular conductors are governed by intermolecular interactions and can be drastically sensitive to the pressure (including chemical pressure) if they are situated near the phase boundary and are soft enough to allow appreciable changes of molecular arrangement and orientation. In contrast to the conventional hydrostatic pressure method, recent development of the uniaxial stress and strain methods have enabled selective and anisotropic regulation of the intermolecular interactions and provided a powerful means to search for novel electronic states.¹ The applied pressure would be more efficient in narrow-band systems where small changes of molecular arrangement and orientation can affect their band structures drastically. A series of anion radical salts based on the metal dithiolene complex $\text{Pd}(\text{dmit})_2$ [dmit=1,3-dithiol-2-thione-4,5-dithiolate; Fig. 1(a)] form one of the most attractive categories of molecular conductors.² Most of them are Mott insulators associated with a narrow and half-filled band at ambient pressure and exhibit a variety of physical properties including superconductivity under hydrostatic pressure. This pressure effect strongly depends on the choice of the closed-shell counter cation. For example, six β' -type anion radical salts of $\text{Pd}(\text{dmit})_2$ with tetrahedral cations $(\text{CH}_3)_4\text{Z}^+$ and $(\text{C}_2\text{H}_5)_2(\text{CH}_3)_2\text{Z}^+$ ($\text{Z}=\text{P}, \text{As}, \text{Sb}$) display various kinds of electronic states under pressure.³ The low-temperature ground state of the $(\text{CH}_3)_4\text{Z}$ ($\text{Z}=\text{P}, \text{As}$) salts remains nonmetallic even at the highest pressure. The $(\text{CH}_3)_4\text{Sb}$ and $(\text{C}_2\text{H}_5)_2(\text{CH}_3)_2\text{P}$ salts exhibit pressure induced superconductivity, and turn nonmetallic under higher pressures. The $(\text{C}_2\text{H}_5)_2(\text{CH}_3)_2\text{Z}$ ($\text{Z}=\text{As}, \text{Sb}$) salts easily turn metallic under pressure, but show neither superconductivity nor high-pressure nonmetallic state. The replacement of the counter cation slightly changes the molecular arrangement and significantly affects the intermolecular interactions. This cation effect lets us infer that the uniaxial strain would be quite effective on this strongly correlated system. In order to ex-

amine the uniaxial strain effect, we first undertook $\beta'-(\text{CH}_3)_4\text{As}[\text{Pd}(\text{dmit})_2]_2$ (abbreviated as TMA salt).⁴ Although the TMA salt remains nonmetallic under hydrostatic pressure, this salt is situated close to the high-pressure superconductor $(\text{CH}_3)_4\text{Sb}$ salt. We report here a remarkable result: the uniaxial strain along the crystallographic b axis induces superconductivity, while small strain along both the a - and c -axis directions effectively enhances the nonmetallic behavior.

Single crystals of the TMA salt were obtained by the air oxidation of $[(\text{CH}_3)_4\text{As}]_2\text{Pd}(\text{dmit})_2$ in an acetone solution containing acetic acid at 5 °C. X-ray diffraction data at room temperature (RT) and 20 K were collected by an imaging plate type Weissenberg camera (MAC Science DIP320V) equipped with a closed-cycle helium refrigerator (DAIKIN Co. V210CSG-UCM). Graphite monochromated Mo $K\alpha$ radiation was supplied by a 21 kW-rotating anode. The structures were solved by a direct method and refined by a full matrix least-squares method. The final R and R_w are 0.0487, 0.0658 for the RT structure and 0.0453, 0.0781 for the 20 K structure, respectively. For the tight-binding band calculation, the extended Hückel molecular orbital calculations were performed. The transfer integral (t) was estimated from the overlap integral (S) by the approximation, $t \approx \epsilon S$ ($\epsilon = -10$ eV, ϵ is a constant with the order of the orbital energies of frontier orbitals). Static magnetic susceptibilities were measured over 5–300 K at the magnetic field of 1 T on randomly orientated single crystals with a Quantum Design MPMS magnetometer. The d.c. resistivity measurements were performed with the standard four-probe method. Electrical contacts were obtained by gluing four gold wires (15 μm diameter) to the crystal with carbon paste. The current direction was parallel to the b axis. Uniaxial strain was applied using the epoxy-crystal method.¹ The samples embedded in the epoxy (Stycast # 1266 and catalyst B) were inserted in a Cu-Be clamp cell. Three samples with different orientations were mounted around the center of the cell to be measured

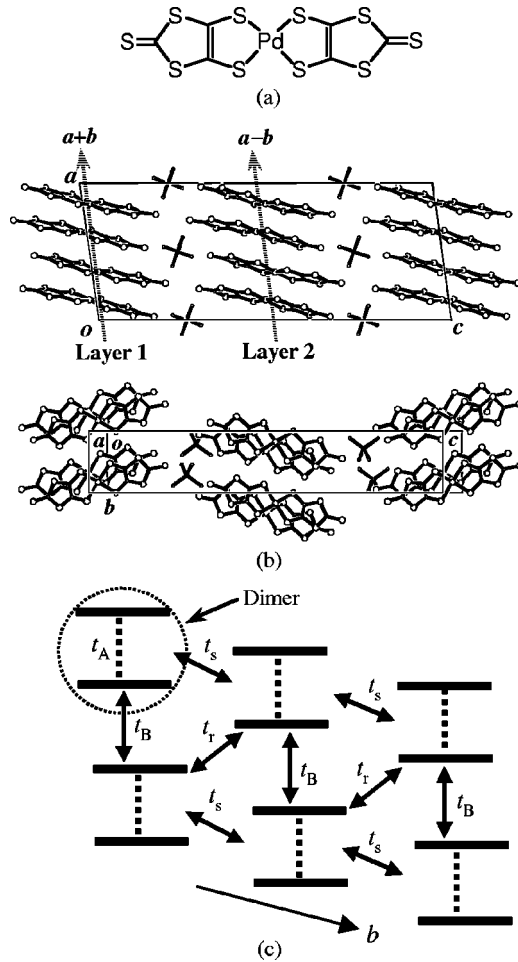


FIG. 1. (a) Molecular structure of $\text{Pd}(\text{dmit})_2$. (b) Crystal structure of β' -(CH_3) $_4\text{As}[\text{Pd}(\text{dmit})_2]_2$. (c) Schematic end-on projection of the conduction layer, where transfer integrals t_A , t_B , t_r , t_s are 448.3, 34.0, 22.7, 32.4 meV (RT) and 485.5, 42.1, 24.4, 32.8 meV (20 K).

simultaneously for three different strain directions. The maximum pressure applied to the sample-head was 15 kbar at room temperature.

Figure 1(b) illustrates the crystal structure of the TMA salt. This crystal belongs to the monoclinic system with the space group $C2/c$. The unit cell consists of two crystallographically equivalent $\text{Pd}(\text{dmit})_2$ layers (I and II), separated from each other by a cation layer. These two layers are interrelated by the glide plane. Strongly dimerized $\text{Pd}(\text{dmit})_2$ molecules stack along the $\mathbf{a} + \mathbf{b}$ direction in Layer I and along the $\mathbf{a} - \mathbf{b}$ direction in Layer II. Within each layer, $\text{Pd}(\text{dmit})_2$ units are connected through intermolecular $\text{S} \cdots \text{S}$ contacts shorter than the sum of the van der Waals radii (3.60 Å) to form a two-dimensional conduction network parallel to the ab plane.

At ambient pressure, the TMA salt has rather low RT resistivity, but exhibits a nonmetallic behavior with lowering temperature.⁴ At the insulating state (20 K), no satellite reflection indicating formation of a superstructure could be observed. The temperature-dependent paramagnetic susceptibility with the RT value of 4.6×10^{-4} emu mol $^{-1}$, forms a

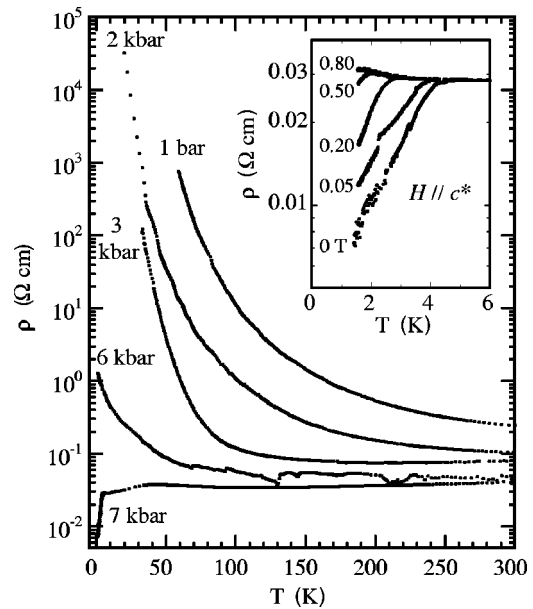


FIG. 2. Temperature-dependence of the resistivity (ρ) under the uniaxial strain along the b axis. The inset shows the resistivity under the magnetic field parallel to the c^* direction at 7 kbar.

broad maximum around ca. 120 K and shows a clear bend around 35 K, below which the susceptibility remains almost constant. The presence of a long-range magnetic ordering below 35 K has been confirmed by an electron spin resonance study.⁵ These results suggest an antiferromagnetic transition at 35 K.

Under hydrostatic pressure, a metal-like region appears and is extended continuously with increasing pressure, but the low-temperature insulating state cannot be suppressed even at the highest pressure (17 kbar).⁶ Under the uniaxial strain, the conducting behavior shows drastic change. When the uniaxial strain along the b axis is applied, the nonmetallic behavior is readily suppressed and an abrupt drop of the resistivity occurs at 4 K under 7 kbar (Fig. 2). As shown in the inset of Fig. 2, recovery of the resistivity by the applied magnetic field has indicated that this is superconductivity induced by the uniaxial strain. This superconductivity can be observed up to 9 kbar. The transition temperature decreases with increasing pressure. Above 10 kbar, slight upturn of the resistivity is observed in the lowest temperature region. It is quite interesting that small strain around 2 kbar along both the a - and c -axis directions effectively enhances the nonmetallic behavior (Fig. 3). With further increase of the strain, the nonmetallic behavior is suppressed, but still remains even at 15 kbar. These observations are different from those under the hydrostatic pressure and the uniaxial strain along the b axis.

For interpretation of these results, it is useful to summarize the characteristics of the present system. The conduction band of the ordinary molecular conductors based on acceptor molecules is formed by the LUMO (lowest unoccupied molecular orbital). In the $\text{Pd}(\text{dmit})_2$ -based conductors, however, the conduction band originates from the HOMO (highest occupied molecular orbital) of the $\text{Pd}(\text{dmit})_2$ molecule.⁷ This is due to a small energy gap (ΔE) between the HOMO and

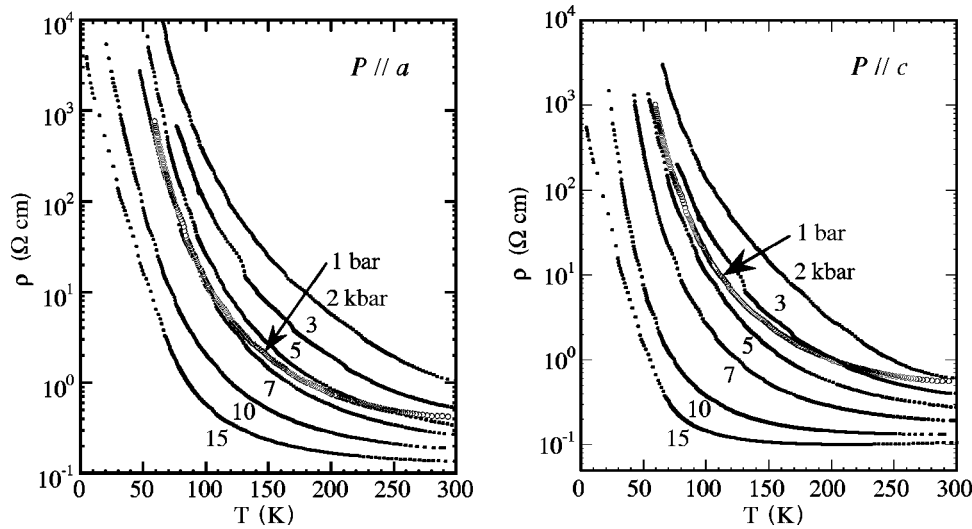


FIG. 3. The uniaxial strain effect along the a and c axis directions on the resistivity (ρ).

LUMO in the $\text{Pd}(\text{dmit})_2$ molecule and the strong dimerization in the crystal. The dimerization of the $\text{Pd}(\text{dmit})_2$ molecules separates each of two bands originated from HOMO and LUMO into the bonding (ψ_{HOMO}^+ and ψ_{LUMO}^+) and antibonding (ψ_{HOMO}^- and ψ_{LUMO}^-) bands. When the generated dimerization gap is large enough compared with ΔE , the HOMO(ψ_{HOMO}^-)-LUMO(ψ_{LUMO}^+) band inversion occurs. This is the case of the TMAs salt.⁸ In the TMAs salt with the formal charge of $-1/2$, the ψ_{HOMO}^- band is half-filled. If the on-site Coulomb interaction (U) is sufficiently larger than the band width (W), the system behaves as a Mott insulator. Indeed, transport and magnetic properties, coupled with the absence of the superstructure in the insulating phase, indicate that the TMAs salt is the Mott insulator under ambient pressure. Although the ψ_{LUMO}^+ band is located near the ψ_{HOMO}^- band and the possibility of the HOMO-LUMO band overlap was proposed, recent x-ray crystal structure analysis for the isostructural $(\text{C}_2\text{H}_5)_2(\text{CH}_3)_2\text{P}$ salt under (hydrostatic) pressure has suggested that the HOMO-LUMO band overlap does not occur and the HOMO band remains the conduction band even under pressure.⁹ When the intradimer interaction is strong, the system can be considered to consist of dimers and one can extract the essence by taking each dimer as an effective unit. Figure 1(c) displays a distorted triangular network of interdimer interactions. This kind of dimer lattice is also considered as a model of the organic superconductors κ -(BEDT-TTF)₂X (X: monoanion) where strong correlation plays an important role.¹⁰ In the κ -type organic superconductors, however, the unit cell contains only one conduction layer where the BEDT-TTF dimers are rotated by about 90° with respect to each other to form a checkerboard-like arrangement. This difference in the packing motif of the dimers would lead to different type of modification of the interdimer interactions under pressure.

As for the TMAs salt, two branches of the conduction HOMO band associated with Layers I and II can be approximately described as follows; $E_{\text{I}}(\mathbf{k}) = 2.0[t_{\text{B}} \cos \mathbf{k} \cdot \mathbf{a}_{\text{p}} + t_{\text{r}} \cos \mathbf{k} \cdot (\mathbf{a}_{\text{p}} - \mathbf{b}_{\text{p}}) + t_{\text{s}} \cos \mathbf{k} \cdot \mathbf{b}_{\text{p}}]$ and $E_{\text{II}}(\mathbf{k}) = 2.0[t_{\text{B}} \cos \mathbf{k} \cdot (\mathbf{a}_{\text{p}} - \mathbf{b}_{\text{p}}) + t_{\text{r}} \cos \mathbf{k} \cdot \mathbf{a}_{\text{p}} + t_{\text{s}} \cos \mathbf{k} \cdot \mathbf{b}_{\text{p}}]$, where the C-centered monoclinic cell is reduced to the primitive one as $\mathbf{a}_{\text{p}} = (\mathbf{a}$

$+ \mathbf{b})/2, \mathbf{b}_{\text{p}} = \mathbf{b}, \mathbf{c}_{\text{p}} = \mathbf{c}$. The interdimer transfer integrals t_{B} , t_{r} , and t_{s} determine the dispersion of the energy band, while the effective on-site Coulomb energy on the dimer (U_{eff}) is approximately proportional to the intradimer transfer integral t_{A} in the $U \rightarrow \infty$ limit.¹¹ In the β' -type salts, there is a relation $t_{\text{A}} \gg t_{\text{B}} \approx t_{\text{s}} > t_{\text{r}}$. The band width W is determined mainly by the two larger interdimer transfer integrals t_{B} and t_{s} , and t_{r} governs anisotropy of the band structure. At room temperature, the $t_{\text{r}}/t_{\text{B}}$ ratio is 0.67 which is smaller than that for the high-pressure superconductor, the $(\text{C}_2\text{H}_5)_2(\text{CH}_3)_2\text{P}$ salt ($t_{\text{r}}/t_{\text{B}} = 0.82$). Fermi surface obtained by the tight-binding band calculation consists of two equivalent cylinders associated with $E_{\text{I}}(\mathbf{k})$ and $E_{\text{II}}(\mathbf{k})$. Each of them has an elliptic cross section.

At the low-temperature insulating state (20 K), the lattice parameters a , b , and c decrease while the β angle increases. The cell volume becomes smaller of about 3% from RT to 20 K. At 20 K, all transfer integrals are enhanced. The anisotropy of the interdimer interaction is enhanced in the low-temperature insulating state ($t_{\text{r}}/t_{\text{B}} = 0.58$). The calculated Fermi surface exhibits more distorted elliptic cross sections at 20 K. It should be noted that the intradimer interaction t_{A} is fairly enhanced. This feature is also observed in the crystal of the $(\text{C}_2\text{H}_5)_2(\text{CH}_3)_2\text{P}$ salt under high-pressure and suggests that U_{eff} in the β' -type $\text{Pd}(\text{dmit})_2$ salts can be variable in response to temperature and pressure.⁹

We now discuss an origin of the unusual uniaxial strain effect. The interdimer interactions can be classified into two categories: intracolumn (t_{B}) and intercolumn (t_{r} and t_{s}) types. A significant structural feature of the β' -type salts is that the unit cell contains two conduction layers. These layers are crystallographically equivalent but are different in the stacking direction of the dimers. The uniaxial strain affects each layer differently except for special directions. One of the special directions is along the b axis. In both layers, the $\text{Pd}(\text{dmit})_2$ dimers are repeated along the b ($=b_{\text{p}}$) axis in a side-by-side fashion [Fig. 1(c)]. Thus, the decrease in b would enhance mainly the intercolumn interactions t_{r} and t_{s} within each layer, which leads to an enhancement of the band width W . As in the case of κ -(BEDT-TTF)₂X, one of criteria

for the Mott transition is the electron correlation parameter, U_{eff}/W .¹² Naively speaking, the most simple explanation for the metallic behavior induced by the b -axis strain is a reduction of this parameter. An important point is that the b -axis strain leads to the best lattice distortion for the enhancement of the intercolumn interaction. On the other hand, the crystallographic a and c axes are orthogonal to the b axis, and thus the uniaxial strain along these directions, basically, should have the smallest effect on the intercolumn interactions. The uniaxial strain along the a axis also has the equivalent effect on each conduction layer. Since normals of the Pd(dmit)₂ molecular planes are at rather small angles ($\pm 30^\circ$) to the a axis, the reduction in a affects mainly the intra-column interactions t_A and t_B . Notably, the uniaxial strain along the a axis induces the enhanced nonmetallic behavior at the low-pressure region. This is one of the most unusual observations and suggests that an enhancement of the intradimer interaction t_A which leads to an increase of U_{eff}/W is predominant in this pressure region. Since the non-

metallic behavior is suppressed upon further increase of the strain, U_{eff} should be in competition with W which is enhanced by t_B . The uniaxial strain effect along the c axis is similar to that along the a axis, which is also unusual. This appears due to the worst strain configuration for the enhancement of the intercolumn interactions and an inclination of the molecular plane out of the c axis (the normal is at an angle of 72° to the c axis).

In conclusion, the electronic state of the Pd(dmit)₂ salts based on the narrow, two-dimensional, and half-filled HOMO band is very sensitive to the intra- and interdimer interactions and can be controlled by the uniaxial strain method. In this sense, the Pd(dmit)₂ system is a unique playground of the strong correlation physics.

This work was partially supported by a Grant-in-Aid for Scientific Research on Priority Areas (No. 10149103 *metal-assembled complexes*) from Ministry of Education, Science, Sports and Culture, Japan.

*Corresponding author. E-mail address: reizo@postman.riken.go.jp

¹C.E. Campos, J.S. Brooks, P.J.M. van Bentum, J.A.A.J. Perenboom, J. Rook, S.J. Klepper, and M. Tokumoto, *Rev. Sci. Instrum.* **66**, 1061 (1995); M. Maesato, Y. Kaga, R. Kondo, and S. Kagoshima, *ibid.* **71**, 176 (2000).

²For a review, see P. Cassoux, L. Valade, H. Kobayashi, A. Kobayashi, R.A. Clark, and A. Underhill, *Coord. Chem. Rev.* **110**, 115 (1991); A. Kobayashi and H. Kobayashi, in *Handbook of Organic Conductive Molecules and Polymers* Vol. 1, edited by H.S. Nalwa (John Wiley & Sons Ltd, 1997) p. 249.

³R. Kato, Y.-L. Liu, Y. Hosokoshi, S. Aonuma and H. Sawa, *Mol. Cryst. Liq. Cryst. Sci. Technol., Sect. A* **296**, 217 (1997); R. Kato, K. Yamamoto, Y. Kashimura, Y. Okano, and S. Aonuma, *Synth. Met.* **103**, 2020 (1999).

⁴A. Kobayashi, H. Kim, Y. Sasaki, K. Murata, R. Kato, and H. Kobayashi, *J. Chem. Soc., Faraday Trans.* **86**, 361 (1990).

⁵T. Nakamura, T. Takahashi, S. Aonuma, and R. Kato, *J. Mater.*

Chem. **11**, 2159 (2001).

⁶T. Naito, Ph.D. thesis, University of Tokyo, 1995.

⁷E. Canadell, I.E.-I. Rachidi, S. Ravy, J.P. Pouget, L. Brossard, and J.P. Legros, *J. Phys. (France)* **50**, 2967 (1989); T. Miyazaki and T. Ohno, *Phys. Rev. B* **59**, R5269 (1999).

⁸H. Tajima, T. Naito, M. Tamura, A. Kobayashi, H. Kuroda, R. Kato, H. Kobayashi, R.A. Clark, and A.E. Underhill, *Solid State Commun.* **79**, 337 (1991).

⁹J. Yamaura and R. Kato, *Mol. Cryst. Liq. Cryst. Sci. Technol., Sect. A* (to be published).

¹⁰K. Kanoda, *Hyperfine Interact.* **104**, 235 (1997).

¹¹M. Mori, K. Yonemitsu, and H. Kino, *Mol. Cryst. Liq. Cryst. Sci. Technol., Sect. A* **341**, 549 (2000). This seems similar to the case of the κ -type BEDT-TTF salts. In the TMAs salt, however, the situation is more complicated because two orbitals (HOMO and LUMO) should be considered.

¹²H. Kino and H. Fukuyama, *J. Phys. Soc. Jpn.* **65**, 2158 (1996).